Chapter 2

AuNP/GO/PEDOT-PSS based immunosensor probes for detection of serum *Immunoglobulin G* (*IgG*)

In Chapter 1, the background and scope of various materials for fabrication of electochemical senors has been reviewed. The role of conducting polymer and 2D layered materials has also been highlighted with their potential applications in the field of sensing. In this chapter, we discuss the development of label free, sensitive, and selective, capacitive immunosensors based on conducting polymer (PEDOT-PSS) and graphene oxide (GO) composite decorated with gold nanoparticles (AuNPs). The composite electrode was fabricated by performing electrochemical polymerization of monomer (EDOT) in presence of GO, keeping PSS as dopant and covered with chemically inert AuNPs. The composite electrode has been studied by using various characterization techniques to understand the composition and morphology. To investigate the electrochemical properties of modified electrodes CV and EIS were employed. Immunosensor fabrication was accomplished by immobilizing mouse IgG over the synthesized electrodes. Afterwards, specific interactions of antibody-analyte for the electrodes were monitored directly via transient capacitance measurements at low and medium frequencies. The AuNP/GO/PEDOT-PSS electrode seems stronger mechanically while offering higher applicability as sensor.

2.1. Introduction

Prior to therapeutics, the role of diagnostic tests in medical care is extremely important. Chapter 1 elucidates the essence of electrochemical sensors and scope of different materials for fabrication of a better-performing sensor. Various nanostructured materials and composites are being explored for cost effective and reliable electrochemical biosensors. The role of conducting polymer and its composite nanostructures for developing an effective transducer has been discussed in section 1.4. PEDOT-PSS is a mixed electron-ion conducting polymer consisting of interconnected conducting PEDOT-rich grains and insulating PSS-rich fibers. PEDOT-PSS comprises two phases of the bulk showcasing relatively *p*-type ionic conductivity [137]. During electrochemical process, the ions are able

to adsorb on these grains resulting in electric double layer (EDL) at the interfaces. PEDOT-PSS is an organic macromolecule that shows potential applicability in electrochemical sensing. Whereas, poor conductivity (~ 0.2 S/cm in pristine form) and slow carrier mobility are the major drawbacks associated with this polymer. The carrier mobility of such conducting polymers can be improved by incorporation of graphene derivatives. This enhancement in mobility arises due to the ordered packing of the graphene sheets with polymer chain and interfacial π–π interaction [138]. Moreover, the biocompatible AuNPs can further modulate the conductivity and catalytic activity over a wide range making it deployable for electrochemical sensing. To date, several works have been carried out on PEDOT-PSS based biosensor reporting different material engineering techniques and detection strategies [139-141]. To be mentioned, impedimetric detection stands out to be an emerging avenue offering rapid, label free and point-of-care detection. The impedimetric response offered by PEDOT-PSS can be utilized for fabrication of impedimetric biosensors with wide detection range. The porous microstructure of PEDOT-PSS offers high surface area and presence of PSS as dopant can aid easy surface functionalization strategy with tailored properties [142].

Here, we report about the fabrication and optimization of sensitive and cost effective AuNP/GO/PEDOT-PSS nanoparticle composite electrode for detection of specific antigen-antibody interaction with great reliability. Incorporation of graphene oxide (GO) has been reported to stabilize the charge transport layers of the PEDOT-PSS. The GO possesses relatively poor conductivity than graphene but the presence of the oxidizing functional groups on its surface makes it suitable for the efficient immobilization of the biomolecules by covalent linkage [143]. It is expected that, deposition of a layer of AuNPs over the electrode can further enhance the carrier transport mechanism. Also, the presence of GO and AuNP in the polymer film might offer better mechanical strength against dissolution of the material in the aqueous electrolyte.

2.2 Experimental

2.2.1. Synthesis of PEDOT-PSS/ITO electrode

At first, PEDOT-PSS was electrochemically deposited over the ITO coated glass substrate (1.5cm×1cm) by using a three-electrode setup in electrochemical workstation. Electrodeposition was performed by cyclic voltammetry (CV) method using Ag/AgCl as reference electrode, a platinum wire as counter electrode and the ITO as working electrode. After arrangement of the experimental setup, all the electrodes were partially dipped (upto

an area of 1cm×1cm) in the as prepared electrolyte. For preparing the electrolyte, 0.1 M of EDOT monomer was dissolved in acetonitrile along with 5% (w/w) PSS and 0.05 M lithium perchlorate. Then the mixture was sonicated for 10 minutes to obtain a uniform solution. For the electro-polymerization of PEDOT-PSS over ITO substrate, 15 cycles of CV were performed at 20 mV/s scan rate by varying the potential under -0.2 V to 1.1 V w.r.t Ag/AgCl. Finally, the appearance of uniform blackish blue colour film over the ITO substrate indicated the successful deposition of PEDOT-PSS polymer. The prepared electrode was then dried at room temperature and stored in the desiccator until further use.

2.2.2. Synthesis of graphene oxide

Graphene oxide was synthesized by following the procedure of modified Hummer's method [144]. At first 3 g graphite powder was added to 100 mL of sulphuric acid, then the solution was kept at constant stirring for a few minutes and 1.5 g of $NaNO_3$ was added simultaneously. Subsequently the mixture was taken in an ice bath to keep the temperature below 20^0C and then 9 g $KMnO_4$ was added gently to the mixture under vigorous stirring. The bath was removed and brought the suspension to 27^0C $\pm 3^0$C and kept for 30 minutes under stirring. After the reaction proceeds, the colour of the solution became dark brown-green and then 140 mL of DI water was added drop wise with constant evolution of brown fumes and the solution was kept at 95^0C for 10 minutes. To remove the excess $KMnO_4$, 20 mL H_2O_2 was added to the solution. As the solution became brown, 420 mL of DI water was further added to the mixture. HCl and DI water was added in 3:1 ratio and centrifuged at 5000 rpm for 7 minutes to separate out liquid from solid and to remove the supernatant. The remaining residuals were rewashed again with HCl and DI water. The washed graphene oxide was dried at room temperature for 24 hours to yield the graphene oxide powder.

2.2.3. Synthesis of GO/PEDOT-PSS/ITO films

The experimental setup used for the electrodeposition of GO/PEDOT-PSS film over ITO substrate was similar as explained in section 2.2.1. Here, the composite film was synthesized by electro-polymerizing EDOT in presence of PSS and GO. For this, 0.1 M EDOT was dissolved in 20 mL solvent (acetonitrile: DI water = 3:2) along with 0.05 M lithium perchlorate, 5% (w/w) PSS and 50 µL of 1 mg/mL GO dispersed aquous solution. The mixture was sonicated for 30 minutes. The cyclic voltammetry was performed for 26 cycles over a potential window, from -0.2 to 1.2 V w.r.t. the Ag/AgCl at a scan rate of 20

mV/s. In case of electrochemical polymerization, first the monomer EDOT is oxidized to a cationic radical by stripping of one electron from EDOT which can be represented as,

$$EDOT - e^{-} \longrightarrow EDOT^{0+}$$

This oxidized form of EDOT has affinity towards negative charges in the solution. To be mentioned, the GO consists of negatively charged functional groups over its edges and basal plane. So, these cationic $EDOT^{0+}$ radicals can easily get attached over the GO sheets in the solution. Moreover, the PSS chain as a negative dopant also get attached with the thiophene rings of the EDOT. Finally, the $EDOT^{0+}$ radicals that are attached with PSS side-chains and GO sheets, get polymerized to PEDOT-PSS along with GO layers stacked in between the polymer chains and having van der Waals interaction between GO layers and thiophene rings. Diminution in current after insertion of GO in PEDOT-PSS is reported by Anna Osterholm *et al*. [145]. Furthermore, with additional cycles of GO deposition, the current would increase as per the arrow mark in Figure 2.1 (a), suggesting improved conductivity with additional layers of GO/PEDOT-PSS deposited on the electrode under study.

2.2.4. Electrodeposition of AuNPs on to GO/PEDOT-PSS/ITO electrode

To perform the electrodeposition of AuNPs onto the GO/PEDOT-PSS/ITO electrode, we replicated the experimental setup outlined in section 2.2.1 with a minor modification. Here, we have utilized the as-prepared GO/PEDOT-PSS/ITO system as the working electrode, while the electrolyte solution was prepared by dissolving 0.5 mL of 3 mM $HAuCl_4$ in 0.1 M KCl solution.

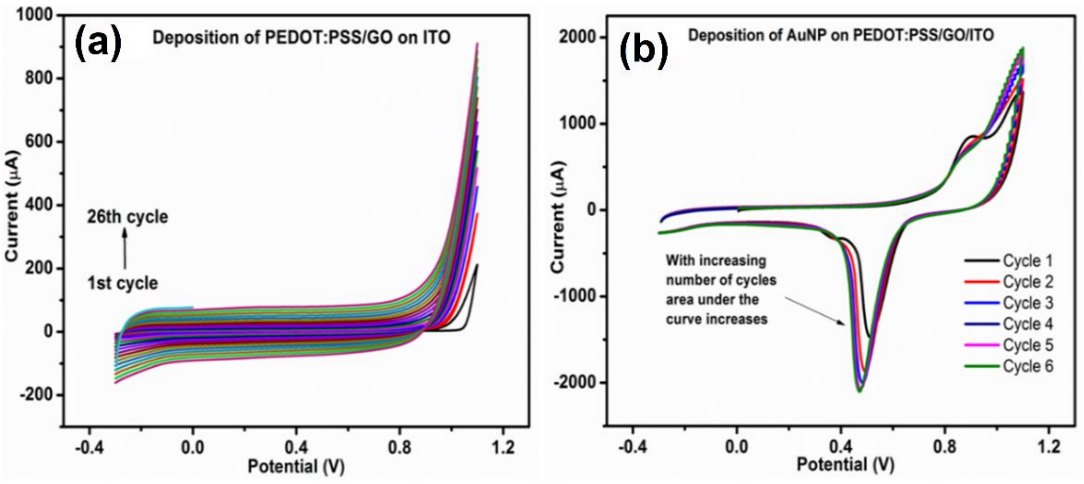

Figure 2.1: (a) Electropolymerization of GO/PEDOT-PSS over ITO, (b) electro-deposition of AuNPs over GO/PEDOT-PSS/ITO film.

The AuNPs were deposited electrochemically on the GO/PEDOT-PSS/ITO electrode by performing CV for 6 cycles under the potential window from -0.2 to 1.2 V w.r.t. Ag/AgCl at a scan rate 10 mV/s [146]. After completion of deposition, the as synthesized AuNP/GO/PEDOT-PSS/ITO electrode was dried at room temperature and stored in desiccator until further use. The deposition curve for AuNPs is shown in Figure 2.1 (b). Here, the sharp reduction peak appearing ~ 0.5 V corresponds to the reduction of $Au^{3+} \rightarrow Au^{0}$ taking place throughout the process.

2.2.5. Fabrication of immunosensor

Antibody (mouse *IgG*) was immobilized over the synthesized composite films by glutaraldehyde cross linking method. Glutaraldehyde is a dialdehyde with two highly reactive aldehydic groups which can bind covalently with different functional groups such as hydroxyl, amine, phenol, thiol, etc. [147]. The as synthesized electrodes are immersed in glutaraldehyde (2% w/v) solution for 1 h such that the hydroxyl groups of PSS and graphene oxide react with aldehydic group to form covalent linkage [148]. After 1h of glutaraldehyde treatment, the solution was removed and the film was rinsed two times with 50 mM PBS (pH 7.4) solution to remove the unbound glutaraldehyde. The film was incubated with mouse *IgG* antibody (250 µg/mL) for 1 h. The reactive -CHO group of glutaraldehyde reacts with the amino group of the antibody and binds covalently, as depicted in Figure 2.2. After removing the excess antibody solution, the film was washed with the PBS buffer. To block the nonspecific sites on the electrode, 40 µL/mL solution of bovine serum albumin (BSA) was added for 1 h. Film was washed with PBS to remove the excess BSA and stored at a temperature of 4°C for further experiment.

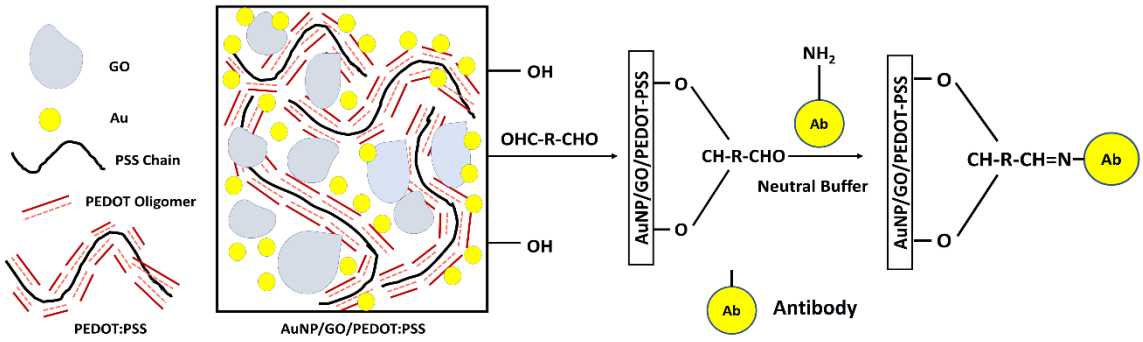

Figure 2.2: Illustration of immobilization of antibody over the surface of AuNP/ GO/PEDOT-PSS/ITO electrode by glutaraldehyde cross-linking

2.2.6. Optimization of pH for AuNP/GO/PEDOT-PSS electrode

To estimate the optimized pH for the Au/GO/PEDOT-PSS based sensor electrode, the voltametric responses are taken by varying the pH values of PBS buffer. Biosensors are used with physiological fluids as electrolytes and 0.05 M PBS (pH=7.4) is highly similar to that of physiological human body fluids. So, 0.05 M PBS was used as the electrolyte for all experiments. The PBS buffer maintains the pH of the solution and prevents cells rupturing due to osmosis. Though the isoelectric point of antigen- antibody molecules are at pH=7 (making them neutral at that pH), the effect of immunocomplex formation which involves hydrogen bonding will change with pH of the buffer electrolyte. In order to separate the effects of electrode substrates with pH of the electrolyte from the effects of antibody interactions, we have carried out the CV measurement for different pH value of the buffer, the results of which are as shown in Figure 2.3. Here, the CV responses of AuNP/GO/PEDOT-PSS is taken by varying the PBS electrolyte pH from 4 to10. We can observe that the current response is maximum at pH=7. And as we move from neutral to acidic solution by lowering the pH from 7 to 4, the AuNP reduction peak height as well as the current response of the CV curve decreases as can be observed in the figure. Similarly, when we go from neutral to basic solution of pH, the current response decreases which can be confirmed from the decrease in the height of reduction peak at 0.5V. From the above plot it is now clear that buffer electrolyte at pH=7 can offer a maximum observable electroactivity.

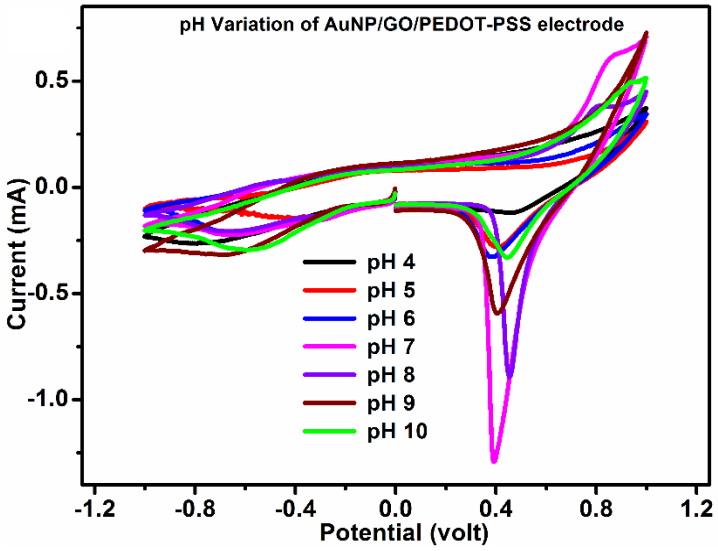

Figure 2.3: Effect of variation of pH; in case of AuNP/GO/PEDOT-PSS substrate electrode

2.3 Results and discussion

2.3.1. Crystallographic study

The PEDOT-PSS, GO/PEDOT-PSS and AuNP/GO/PEDOT-PSS films were deposited over ITO substrate via electrochemical technique as discussed in section 2.2. Afterwards, the as-prepared electrodes were directly loaded in the XRD machine to acquire the powder diffraction patterns. The obtained XRD responses of the three systems are shown in Figure 2.4. In the black XRD response, the broad hump appearing around 25° corresponds to the electrodeposited PEDOT-PSS film [149]. Other significant crystalline peaks appearing at ~ 21.36°, 30.3°, 35.3°, 41.4°, 45.3°, 50.6°, 58.7°, 60.2° are due to the presence of ITO substrate at the base of each electro-deposited systems (ICDD ref No. 00-039- 1058) [150]. In the second system, GO shows its characteristic peak at ~ 13.3° resembling (002) plane with d-spacing value of ~ 0.67 nm [151]. In the third system, the characteristic diffraction peak of AuNPs is observed at ~ 38.2° that corresponds to (111) diffraction plane. Whereas other sharp peaks located at, 2θ = 44.4°, 64.6° and 77.6° signify the (200), (220) and (311) crystal planes of AuNPs (ICDD ref No. 00-004-0784), respectively [152]. The XRD response of the second system indicates the incorporation of GO in the PEDOT-PSS system. Whereas, appearance of Au characteristic peaks in the third system confirms the presence of AuNPs in the GO/PEDOT-PSS system.

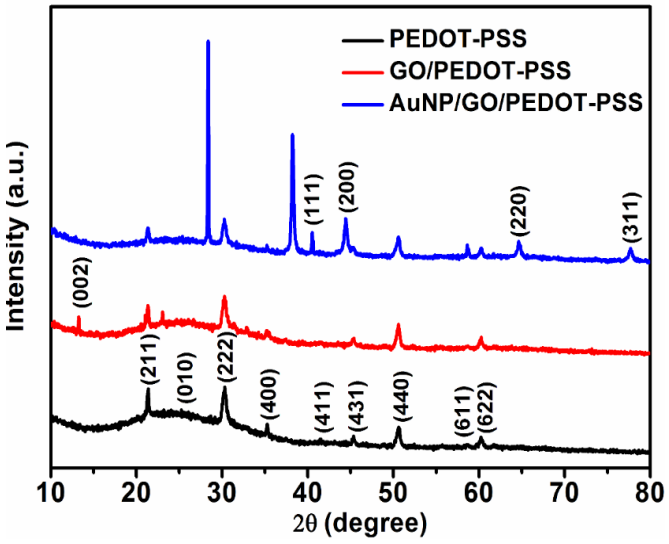

Figure 2.4: XRD patterns of PEDOT-PSS, GO/PEDOT-PSS and AuNP/GO/PEDOT-PSS on ITO electrode

2.3.2. FT-IR analysis

For FT-IR analysis, we have first electrodeposited the PEDOT-PSS, GO/PEDOT-PSS and AuNP/GO/PEDOT-PSS films over the ITO substrate as described in section 2.2. Then the as deposited films were gently peeled out from the ITO glass by using a small spatula. These peeled off film samples were then characterized by FR-IR technique. The FT-IR spectra of all the three systems are shown in Figure 2.5. In pristine PEDOT-PSS, the peaks appearing at ~ 2923 cm^{-1} and 2853 cm^{-1} are due to the asymmetric and symmetric stretching of CH_2 respectively. The notable peak at 1640 cm^{-1} corresponds to symmetric C=C stretching. The peaks located around 1335 cm^{-1} and 1465 cm^{-1} are due to the stretching vibrations of C-C and C=C of the quinoidal structure, that originates from the thiophene ring [153]. Vibrational bands that appeared at, 1199 cm^{-1} and 1080 cm^{-1} are due to the asymmetric stretching of C-O-C in the ethylene dioxy part and symmetric stretching of S=O in SO^{3-} group of PSS, respectively. A band around 978 cm^{-1} is observed due to the deformation in ethylene dioxy ring. The broad absorption peak at 664 cm^{-1} appears due to the C-S stretching of the thiophene ring [154]. In the binary systems of GO/PEDOT-PSS, the evidence of several types of functional groups that are generated by oxidation are confirmed by the FT-IR spectra. The vibration modes appeared between the range 2800–3000 cm^{-1} are due to the C-H stretching mode. Moreover, the shifted peaks at ~ 1331 cm^{-1} and 1638 cm^{-1} are attributed to the vibrational modes of epoxide (C-O-C) and sp^2-hybridized carbon (C=C); respectively. The peak at 1517 cm^{-1} matches with the C-O stretching of alkoxy group [154]. The peaks that appeared in the range of 600-700 cm^{-1} can be attributed to the C-H deformation in the polymer-GO composite. Due to C=C out of plane benzene ring bending of the GO sheets, an absorption peak at 435 cm^{-1} is observed [155]. In the FT-IR spectrum of PEDOT-PSS, the appearance of all vibrational modes at their specific position indicates the adequate formation of the polymer structure. After incorporation of GO in the pristine system, dislocation and suppression of some vibrational modes have been observed indicating the insertion of GO sheets in the polymer backbones as described in section 2.2.3. In the ternary system, shifting and disappearance of some less prominent peaks can be traced in the blue spectrum of Figure 2.5 which is due to the surface-deposition of the AuNPs over the binary system forming AuNP/GO/PEDOT-PSS hybrid nanostructure. The shifting and vanishing of these modes are due to the strain induced within the polymer structures because of GO and AuNP incorporation.

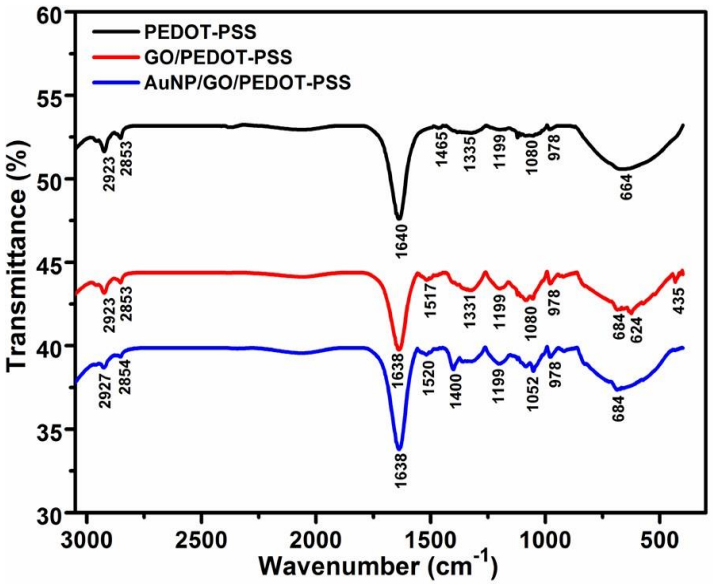

Figure 2.5: FT-IR spectra of PEDOT-PSS, GO/PEDOT-PSS and AuNP/GO/PEDOT-PSS on ITO electrode

2.3.3. Morphological study and elemental analysis

For morphological study, a similar procedure of sample preparation has been followed as mentioned in section 2.3.1. Then the morphological study of the as prepared PEDOT-PSS, GO/PEDOT-PSS, AuNP/GO/PEDOT-PSS electrodes were carried out on an electron microscopy technique. Here, the SEM micrographs of all three electrodes were captured at 2 μm scale range with 5500x magnification. In Figure 2.6 (a), the pristine PEDOT-PSS film shows clusters of about 400 nm size connected by long chains or fibers and appeared to be highly porous. The clusters are presumed to be an aggregation of the PEDOT-rich grain like particles. After addition of GO in the monomer solution, the polymer film is formed by entrapping the GO sheets in between the polymer chains. This results in the formation of smaller clusters as seen in Figure 2.6(b). Figure 2.6(c) depicts the aggregation of AuNPs over the GO/PEDOT-PSS/ITO film, which results in the increase of surface roughness and disappearance of fibrous structure in the film surface. Due to multiple cycles of deposition, these noble metal NPs get agglomerated over the surface of polymer film. The adjacent figure of each micrograph shows the EDX response of the synthesized electrodes. The relative elemental percentage confirms the presence and concentration of different elements in the synthesized film. The EDX spectra of Figure 2.6 (a) characterizes the X-ray emission spectra corresponding to the K-shell transition energy of carbon, oxygen and sulfur that confirms the presence of these constituents in the PEDOT-PSS film. In case of GO/PEDOT-PSS, the relative atomic percentage of oxygen exceeds, which is due to the

presence of the oxygen containing functional groups in the graphene oxide sheets. The deposition of AuNPs over the GO/PEDOT-PSS film is confirmed by the emission spectra corresponding to the M-shell transition energy of Au, as can be seen in the EDX response of Figure 2.6 (c).

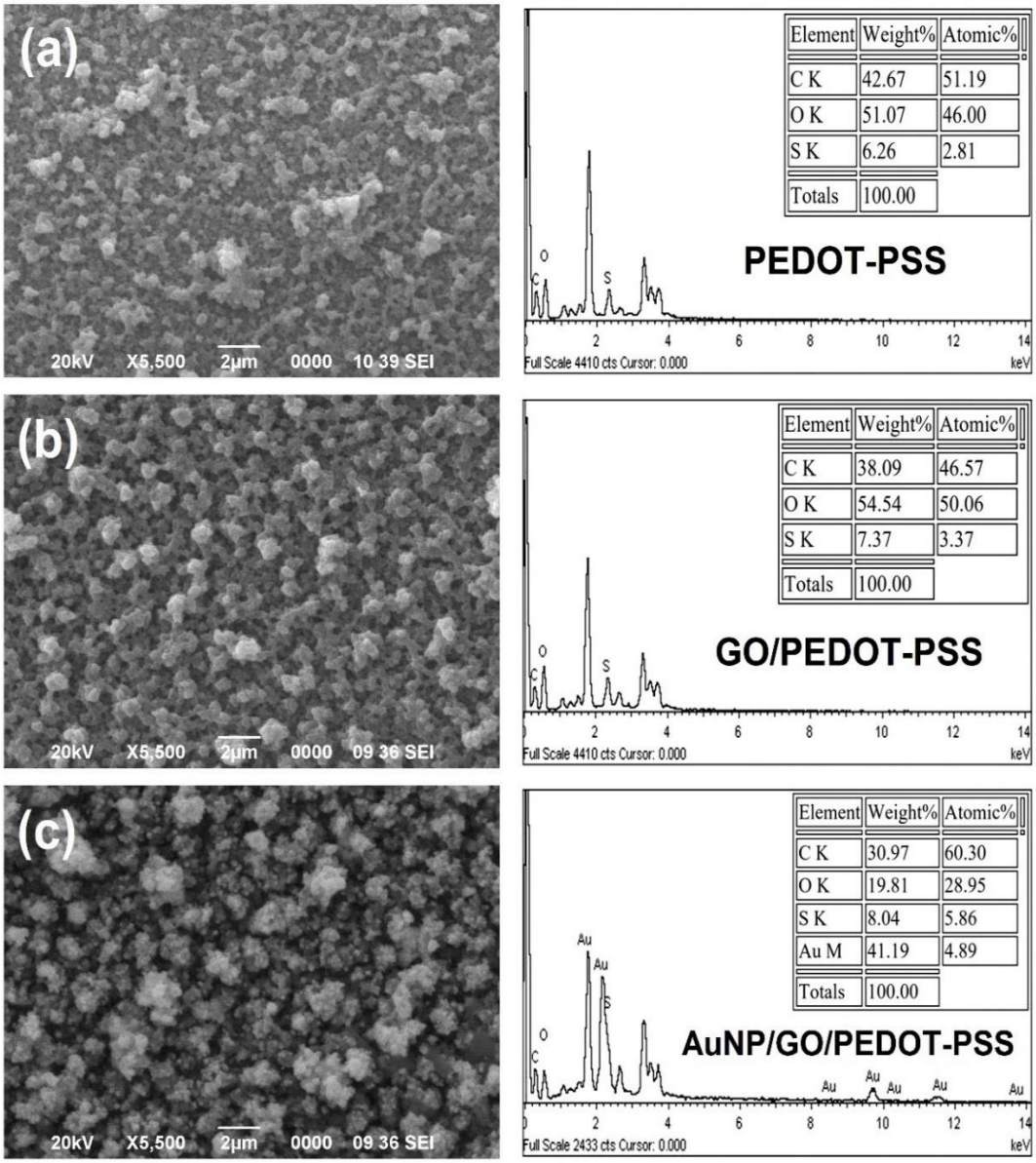

Figure 2.6: SEM micrograph and EDX response of (a) PEDOT-PSS, (b) GO/ PEDOT-PSS, and (c) AuNP/GO/PEDOT- PSS on ITO

2.3.4. Mott-Schottky plot for PEDOT-PSS film

The mismatch in Fermi level at metal-semiconductor contact gives rise to Schottky barrier [156]. Such intimate contact of metal and semiconductors results in the band bending phenomena at the interface giving rise to a depletion region. In our electrochemical setup,

the electrode (W.E.) and electrolyte system can also be considered as analogous to metal-semiconductor system. The bending of bands occurring at the interface of the *p*-type semiconducting electrode has been depicted in Figure 2.7(a)(i). In this figure, E_c and E_v represents the energy level of conduction and valence band, respectively. E_{FS} is the fermi energy level of the *p*-type semiconductor. E_{redox} is the fermi energy level of the electrolyte which typically lies in between the oxidation and reduction potential of the electrolyte. In the figure, the dielectric depletion layer is basically the Helmholtz double layer emerging at the interface. This dielectric interlayer is the cause of capacitive effect in the system. On the other hand, the band bending phenomena gives rise to accumulation of opposite charges at the interface forming junction/depletion region [157]. Besides, these bands can be made flat by applying an external potential called flat band potential (V_{fb}) as shown in Figure 2.7(a)(ii). The value of V_{fb} is equivalent to the difference in fermi energy levels of electrode and the electrolyte, given as $V_{fb} = E_{redox} - E_{FS}$. The capacitance ($C$) vs. applied voltage ($V$) graph of Figure 2.7(a)(iii) shows that if the applied voltage, $V > V_{fb}$, then the value of capacitance decreases due to the widening of the depletion region. The accumulation of the negative carriers at the junction gets saturated at a certain voltage called threshold voltage V_{Th}. Beyond this voltage, the capacitance will remain constant for an ac signal of medium frequency ranging from 1 kHz to few tens of kHz. Whereas, a low frequency signal shows a variation in capacitance as depicted by the dashed curve of Figure 2.7(a)(iii). If the applied potential (V) is further increased, then at $V \sim 2V_{Th}$, the inversion phenomena will occur [158]. This means, the *p*-type semiconductor will behave like *n*-type after reaching this inversion voltage. To obtain a consistent capacitive response along with high carrier mobility in the case of PEDOT-PSS based electrode, we had to optimize the frequency as well as the applied bias voltage for getting a stable response throughout the impedometric detection. At first, Mott-Schottky (M-S) plot was recorded for recognizing the type of carrier and determining the V_{fb} value. The Mott-Schottky equation gives a direct relation between C vs V, as follows:

$$\frac{1}{C^2} = \frac{2}{\varepsilon\varepsilon_0 e A^2 N_D}\left(V - V_{fb} - \frac{k_B T}{e}\right) \qquad (2.1)$$

Here, e is electronic charge, N_D is the density of free or delocalized carriers, V is the applied voltage while V_{fb} indicates the flat band potential, k_B is the Boltzmann constant, and T is absolute temperature [159].

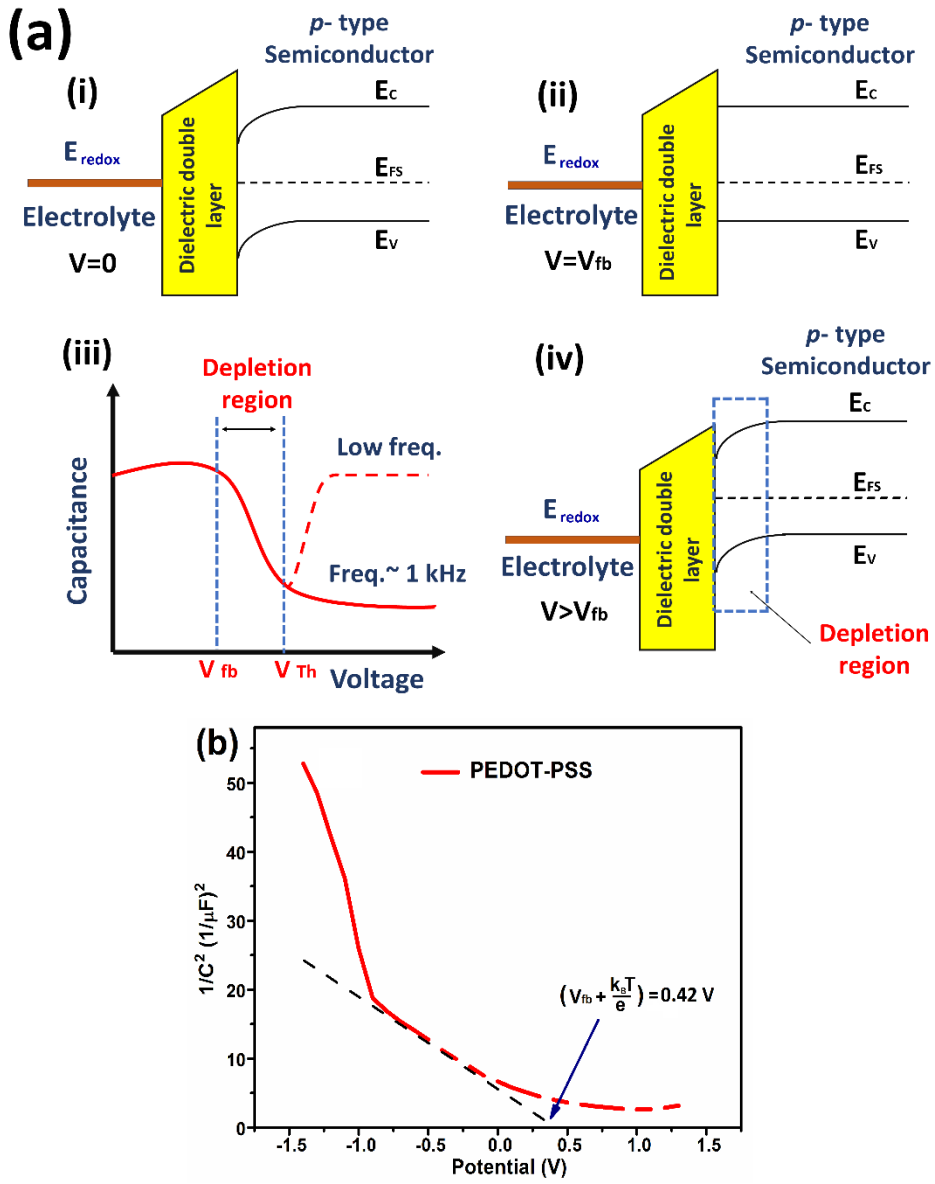

Figure 2.7: (a) Schematic representation of band bending phenomena on electrode-electrolyte junction, (b) Mott-Schottky plot of PEDOT-PSS/ITO

The experiment was performed in the three-electrode system configuration using PEDOT-PSS as working electrode in 0.05 M PBS solution at 1 kHz frequency. The M-S plot obtained for our system is shown in Figure 2.7(b). The negative slope of the graph suggests that *p*-type carrier is present in our system and the flat band potential of PEDOT-PSS film is estimated to be 0.394 V. Besides, the *n*-type semiconductor possesses high carrier mobility and better electronic conductivity offering fast charge transport. So, we intended to use our system as *n*-type semiconductor. To do this, we had applied an inversion potential of 0.8 V w.r.t the reference electrode which facilitates maximum accumulation of electrons at the junction allowing our system to behave as *n*-type semiconductor. Also, use

of 1 kHz signal frequency provides a constant capacitive response when we work beyond the threshold voltage (Figure 2.7(a)(iii)). Based upon the optimized value of the bias potential, a DC bias voltage of 0.8 V was assigned in the single frequency transient plot.

2.3.5. Cyclic voltammetric studies of fabricated PEDOT-PSS GO/PEDOT-PSS/ITO and AuNPs/GO/PEDOT-PSS/ITO electrodes

In this work, all electrochemical measurements were performed on the electrochemical workstation where a platinum wire was used as a counter electrode and Ag/AgCl as reference electrode. However, the PEDOT-PSS/ITO, GO/PEDOT-PSS/ITO and AuNPs/ GO/PEDOT-PSS/ITO based immunosensor electrodes were used as working electrode. The fabrication procedure of the immunosensor has been explained in section 2.2.5. The experimental setup consists of a conical vessel filled with 500 mL of 0.05 M PBS as electrolyte solution. The electrodes were moderately dipped in the reaction vessel as per three-electrode configuration. This experimental setup was further used for performing all the electrochemical measurements (*viz.* CV, EIS and transient capacitance plot) throughout this study.

All the CV responses were taken at a scan rate of 20 mV/s under the potential window of -0.2 to +1.2 V. As shown in Figure 2.8(a), there are high intensity oxidation and reduction peaks (A and C) which have been observed for pristine PEDOT-PSS electrode. The broad redox peaks with high peak potential separation (ΔE_p) indicates the slow electron transfer at the electrode surface, *i.e.*, irreversible process. However, the peak current decreased for GO/PEDOT-PSS modified electrode due to the presence of oxidative groups in GO which results in surface negative charge that lowers the electron transfer by generating barrier towards the flow of electrons [160]. In the Au deposited ternary electrode one reduction peak is observed at, ~ 0.29 V which is due to the reduction of $Au^{(3+)}$ to $Au^{(0)}$ [140]. The electrochemical behaviour of the ITO electrode modified with GO/PEDOT-PSS and AuNPs/GO/PEDOT-PSS before and after immobilization of antibody (Ab, mouse IgG) and after binding with analyte (goat anti mouse IgG) were studied using CV, as shown in Figure 2.8(b) and (c) respectively. In Figure 2.8(b) there is a gradual reduction in the peak current at -0.7 V for the GO/PEDOT-PSS electrode which is due to the slow redox process between the electrolyte and electrode. This is because, the antibody partially blocks the active sites of the electrode after immobilization has taken place, indicating an adsorptive nature of the fabricated electrodes [161]. In case of AuNP/GO/PEDOT-PSS electrode, the sharp reduction peak current at 0.29 V decreases

gradually after each process step and shifts towards 0.25 V after antibody immobilization, as can be seen in Figure 2.8(c). Similarly, the broad reduction peak appeared at -0.5 V also falls gradually with each process step indicating slow electron transfer kinetics. However, after antigen interaction, a broad oxidation peak at -0.15 V appears in the case of both GO/PEDOT-PSS and AuNP/GO/PEDOT- PSS indicating an interfacial charge transfer among the different layers of the modified electrode [162]. Observation of new oxidation peak may be attributed to the slow transfer of charges among the different layers of both pristine and modified electrodes when the antibody binds with antigen. Antigen-antibody interactions mainly involve weak interactions such as hydrogen bonding, steric interactions and electrostatic interactions and these processes are slow since the antigen molecules are huge and binding involves conformational changes.

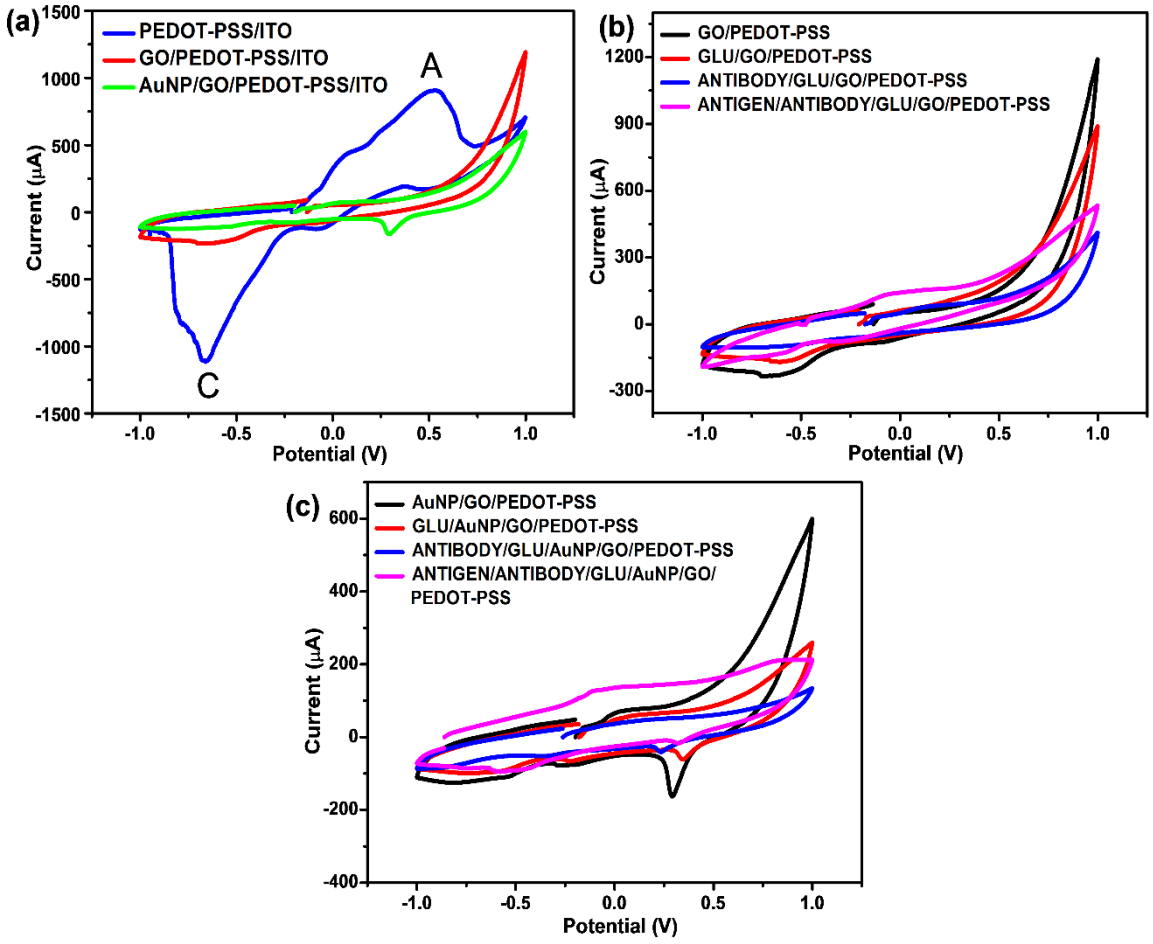

Figure 2.8: (a) CV plots of PEDOT-PSS, GO/PEDOT-PSS, AuNP/ GO/PEDOT -PSS on ITO; Cyclic voltammetry of the (b) GO/PEDOT-PSS and (c) AuNP/GO/PEDOT-PSS sensor after each process step with a total Antigen (*IgG*) concentration of 23.47 µg/mL in 0.05 M PBS buffer.

The weak interactions may cause breaking of some hydrogen bonds from the modified electrode surface altering its surface charge giving rise to broad redox peaks. The study indicates that, though PEDOT-PSS is a good conducting polymer and the GO has high surface area, the conductivity of the modified GO/PEDOT-PSS electrode would decrease after the GO incorporation since the surface charge on GO may form *p-n* junctions with *p*-type PEDOT-PSS. Similarly, introduction of chemically inert, stable AuNPs to the system may form a passive layer which decreases the current further. Here, use of any enzyme labels to stabilize the current response. So, we can't rely on the CV responses to explain the monotonic changes occurred during the different experimental steps. That is why, a careful analysis of the impedance measurements is required to explain the interfacial modifications occurring throughout the sensing experiment.

2.3.6. Characterization of immunosensor using impedance spectroscopy

The electron transfer kinetics between the pristine and modified electrodes over their electrolyte interface were characterized by electrochemical impedance spectroscopy (EIS). The experimental setup and sample preparation procedure for EIS study is similar as explained in section 2.3.5. The EIS was performed in the frequency range 1 mHz to 1 MHz for PEDOT-PSS, GO/PEDOT-PSS and AuNP/GO/PEDOT-PSS deposited ITO electrodes in the PBS solution. The respective impedance spectra for the electrochemical cells with bare electrodes such as PEDOT-PSS, GO/PEDOT-PSS and AuNPs/GO/PEDOT-PSS are shown in Figure 2.9 (a). Whereas, the impedance spectra (Nyquist plot) for GO/PEDOT-PSS and AuNPs/GO/PEDOT-PSS after each process step of the sensor fabrication such as after glutaraldehyde deposition, antibody immobilization and antigen interaction can be found in Figure 2.9 (b) and (c). Here, the dashed curves represent the fitted impedance spectra for the respective electrode systems, and the inset circuit of Figure 2.9 (a) depicts the equivalent Randle circuit used to fit the impedance data. The equivalent circuit remains the same for each composition of the electrode and after each process step for the fabrication of the sensor. In the equivalent circuit, the series resistance R_1 appears due to the solution resistance, Q_2 is constant phase element (CPE) similar to the double layer capacitance (C_{dl}) representing a nonblocking interface. R_2 is charge transfer resistance (R_{ct}) represented by the diameter of the suppressed semicircle at high frequency region. Basically, an increase in R_{ct} value indicates the hinderance in interfacial charge transfer. W_3 is Warburg impedance which arises due to diffusion process in the polymer chain and Q_3

is another CPE which represents the space charge layer either between ITO and PEDOT-PSS, or between PEDOT-PSS and GO, or Au.

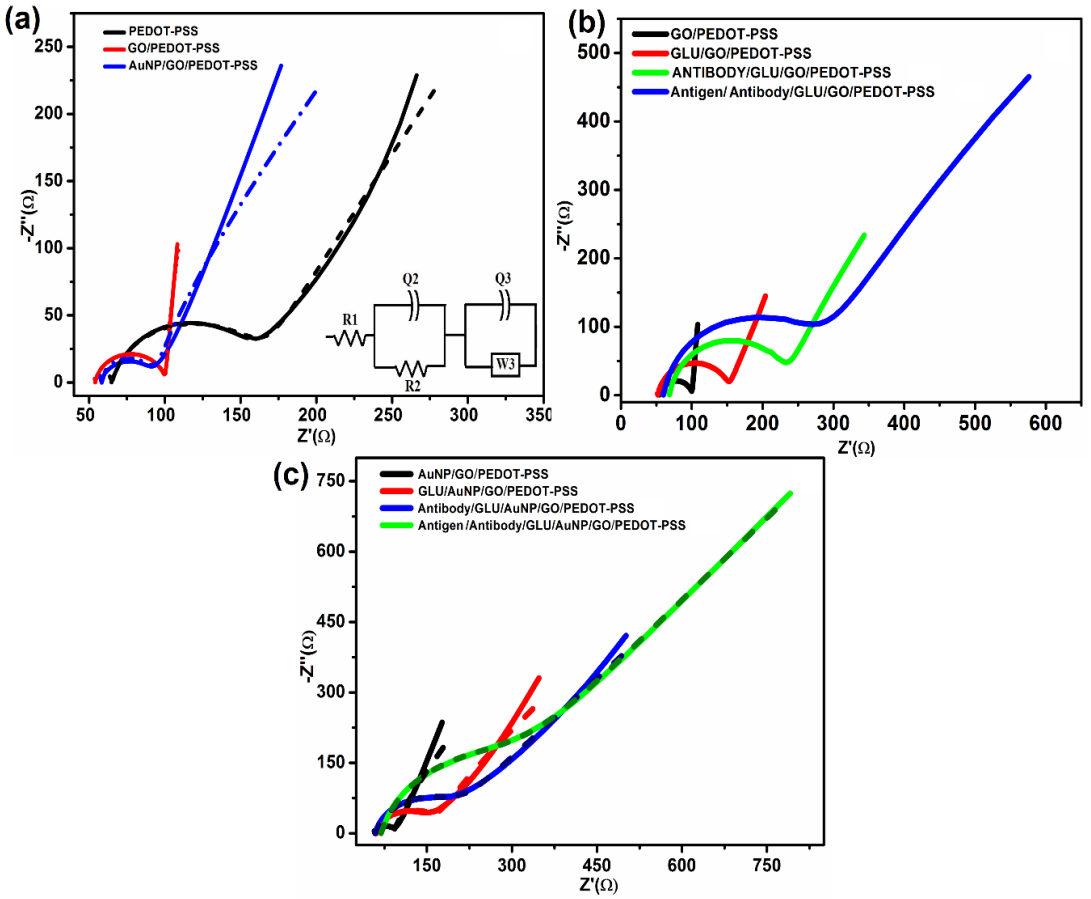

Figure 2.9: (a) EIS plot of PEDOT-PSS, GO/PEDOT-PSS, AuNP/GO/PEDOT-PSS on ITO; Impedance response of the (b) GO/PEDOT-PSS and (c) AuNP/GO/ PEDOT-PSS sensor after each process step with a total Antigen (*IgG*) concentration of 23.47 µg/mL.

The diffusive part comes into action due to the porous/interconnected nature of the conducting polymer film. The diffusive nature diminishes after incorporation of GO and AuNPs in the polymer film. This is confirmed from the significant decrease in the Warburg impedance (W_3) of the modified electrode after incorporation of GO and AuNPs. Table 2.1 shows the fitted parameter values of the equivalent circuit corresponding to all three electrodes. The series resistance does not change much for all the electrodes under study. It is observed that, the R_{ct} value of PEDOT-PSS/ITO is 95.2 Ω which is higher as compared to that of the other two electrode compositions. The R_{ct} value decreases to 34.08 Ω after incorporation of GO and Au in the polymer matrix. This is because, the cross-linked polymer structure forms continuous layer which helps in easier charge transfer and a robust

electrode. The systematic increase in impedance occurring after each process step of the immunosensor fabrication indicating the formation of heterostructures and additional layers at the solid-electrolyte interface which manipulating the dielectric properties of the system.

Table 2.1: Fitted parameters of EIS spectra for the pristine, binary and ternary electrode

Electrode	R_1 **(Ω)**	R_2 **(Ω)**	Q_2 **(×10^{-6}) S.s$^{\eta}$**	Q_3**(×10^{-3}) S.s$^{\eta}$**	W_3 **S.s$^{1/2}$**
PEDOT-PSS	64.79	95.20	15.86 η=0.877	0.692 η=0.760	1455
GO/PEDOT-PSS	54.04	46.69	9.370 η= 0.925	1.404 η=1	1530
AuNP/GO/PEDOT-PSS	58.32	34.08	5.574 η=1	0.409 η=0.913	817.7

For further impedance response analysis, impedance data in Figure 2.9(c) was fitted and the corresponding fit parameters of the equivalent circuit are shown in Table 2.2. We can see that the R_{ct} value of AuNP/GO/PEDOT-PSS increases after glutaraldehyde treatment. Glutaraldehyde as a thin neutral layer is getting bound over the electrode surface resulting in total impedance increase. The R_{ct} value further increases to 120.2 Ω after the addition of antibody (which are neutral at pH=7.4) and BSA. This suggests the successful binding of the antibody layer over the electrode surface (via glutaraldehyde cross-linking) followed by blocking of non-specific sites by BSA. A further increase in the value of R_{ct} is observed after the addition of antigen confirms the antibody-antigen interaction. It is noteworthy that Q_2, or C_{dl} value increases after glutaraldehyde treatment due to the introduction of reactive di-aldehydic groups over the electrode which results in increasing the electroactive area in double layer interface. The slight decrease in Q_2 value after antibody immobilization may be due to the blocking of the redox active sites between the electrode-electrolyte interface by electrically neutral (at pH=7.0) antibody and BSA. However, Q_2 again increases after binding with antigen indicating the presence of surface-active groups in the antibody-antigen complex. Again, the drastic change in Q_3 with η<1 after antibody immobilization and antigen interaction on the modified electrode suggesting the formation of inhomogeneous electrode surface due to the adsorption of these biomolecules. The antigen-antibody interactions are highly specific and the resulting complex forms a dielectric layer. The enhancement in impedance value is due to the

formation of the antigen antibody complex on *Ab* immobilized electrode surface which reduces the redox process between the electrode and electrolyte while charge transfer among the various layers of the working electrode increases as observed in the cyclic voltammetry plots [163]. Moreover, in Table 2.2, increase in the value of W_3 indicated the increase in diffusional impedance after each process which is due to the introduction of porous layers after each process step, mainly due to the conformational changes in antibody-antigen proteins.

Table 2.2: Fitted parameters of the EIS spectra for the ternary electrode (AuNP/GO/ PEDOT-PSS) based sensor after every process step during sensor fabrication.

Electrode	R_1 (Ω)	R_2 (Ω)	$Q_2(\times10^{-6})$ S.s$^{\eta}$	$Q_3(\times10^{-3})$ S.s$^{\eta}$	W_3 S.s$^{1/2}$
AuNP/GO/PEDOT-PSS	58.32	34.08	5.574 η=1	0.4095 η=0.913	817.7
GLU/AuNP/GO/ PEDOT-PSS	61.26	109	18.77 η=0.8529	0.1216 η=1	833.8
BSA/Antibody/GLU/AuNP/GO/PEDOT-PSS	58.96	120.2	15.25 η=0.9093	98.85×10^{-3} η=0.7652	1179
Antigen/BSA/Antibody/GLU/AuNP/GO/ PEDOT-PSS	68.98	172.1	30.49 η=0.9476	73.49×10^{-3} η=0.7961	2174

2.3.7. Detection of the specific antigen

Though we have used a detailed equivalent circuit for fitting the impedance spectra and extracting information about the charge transfer processes in the microstructure, for the ease of separating the capacitive (imaginary impedance) and resistive (real impedance) part in electronics design, impedance of the immunosensor can be assigned as a more general equivalent circuit consisting of a series resistance representing the electrolyte resistance in series with parallel combination of resistance (R_p) and capacitance (C_p). For a label free immunosensor which does not use redox agents or enzymes, the maximum change occurs due to antigen antibody interactions (additional dielectric layer formation at the electrode surface during antigen binding) can be monitored at medium or low frequency transient capacitance measurements in the accumulation bias [164]. The electrode/electrolyte interface works as an electrolytic capacitor. Therefore, detection of antigen is done by

single frequency transient plot of parallel capacitance (C_p) vs. time at a fixed DC bias voltage of 0.8 V (PEDOT-PSS/ITO shows *p*-type conductivity, so we have used an accumulation bias of 0.8 V which will show maximum sensitivity) w.r.t. the reference electrode. The experimental setup for this transient capacitance plot has already been described in section 2.3.5. The capacitive response of the immunosensors were monitored w.r.t. time at two frequencies: 77 Hz and 1 kHz.

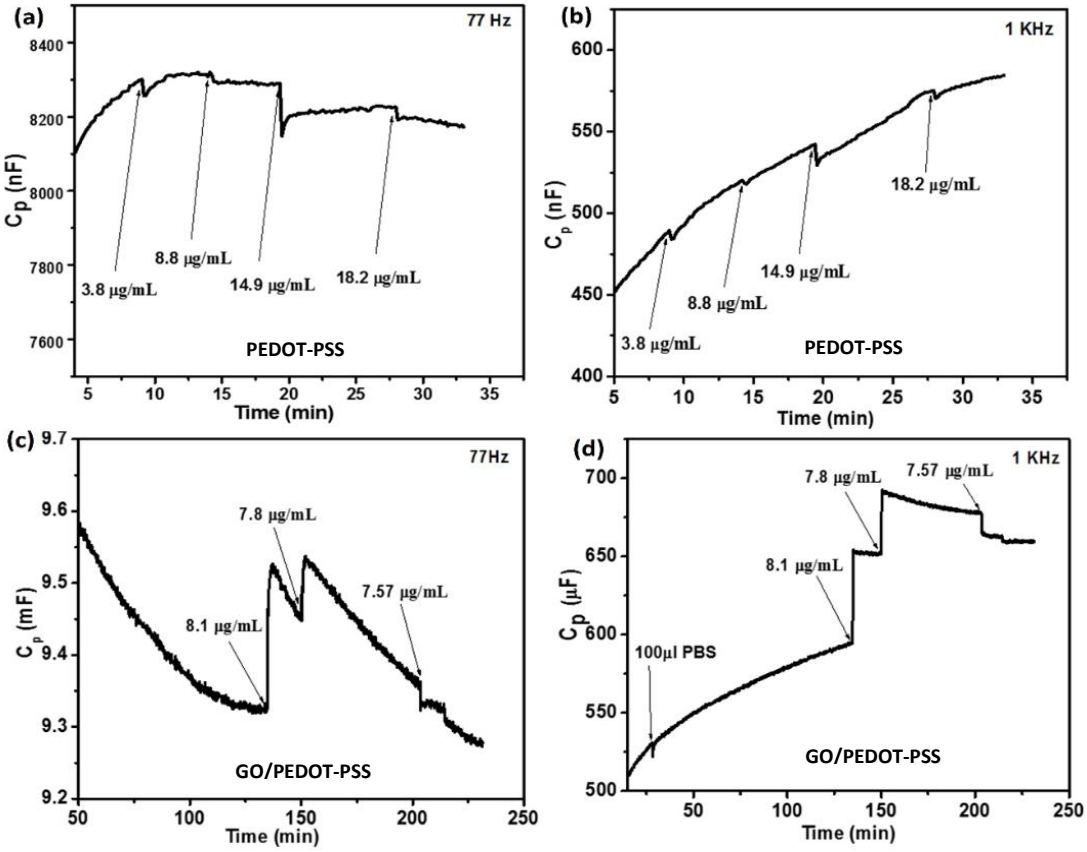

Figure 2.10: C_p vs. time plots of PEDOT-PSS at (a) 77 Hz, (b) 1 kHz frequency, and (b) C_p vs. time plots of GO/PEDOT-PSS based sensors at (c) 77 Hz, and (d) 1 kHz frequency with various concentration of antigen injections.

For transient capacitance measurements, once a stable baseline is obtained for the cell, different amounts of antigenic whole serum were added in the electrolyte at different time intervals and change in capacitive response was observed on each subsequent addition [165]. During antibody antigen interaction, binding of antigen over the immunosensor increases the thickness of dielectric layer between the interface of the electrode and electrolyte that would give rise to a change in the capacitive response in the transient plot [166]. Typical capacitance transients at 77 Hz and 1 kHz for PEDOT-PSS and GO/PEDOT-PSS are given in the Figure 2.10 above. Both these sensors show changes in the transient

capacitance with antigen antibody interaction. The GO/PEDOT-PSS electrode showed enormous, but non-monotonous alternations after few additions of antigen, which makes the sensor less reliable. While for PEDOT-PSS sensor, though the changes were monotonous but not proportional. Transient capacitance plots for Au/GO/PEDOT-PSS measured at both 77 Hz and 1 kHz frequencies are presented in Figure 2.11 (a) and (b). Both the plots exhibit systematic decrease in capacitance with added concentration of antigen. The selectivity of the system is examined by adding higher concentrations of BSA (40 μg/mL) in the electrolyte, which is a nonspecific protein for the immobilized mouse *IgG*. Upon addition of BSA, first the baseline capacitance decreases significantly for 77 Hz frequency response but soon it increases to retain its earlier trend suggesting no interaction with the antibody. This characterizes the selective nature of the immunosensor. However, at 1 kHz, it gives a larger change as in the case of specific antigen additions with different kind of interaction kinetics.

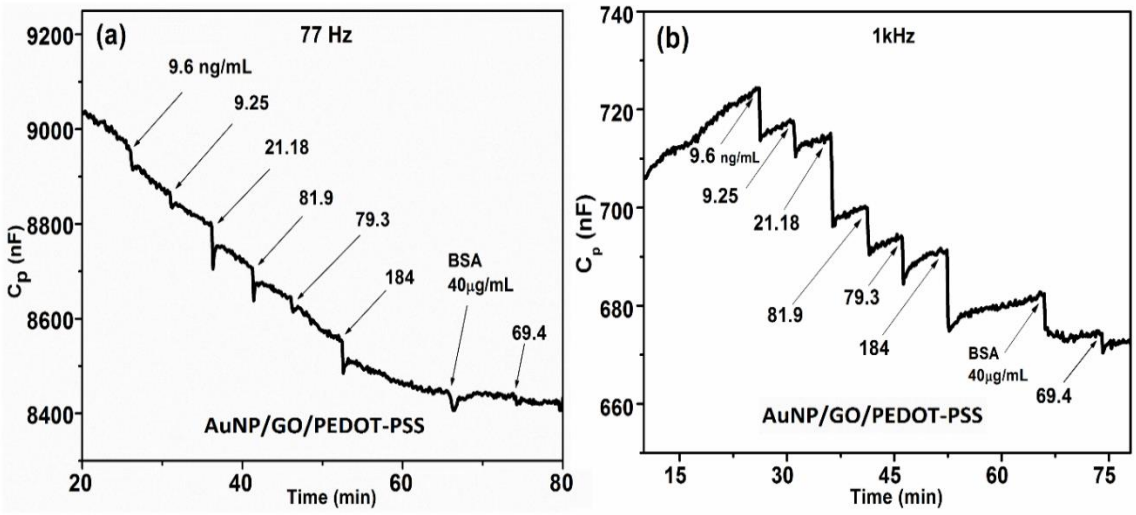

Figure 2.11: C_p vs. time plots of AuNP/GO/PEDOT-PSS sensor with various antigen injections in ng/mL concentrations at different frequencies, (a) 77 Hz, and (b) 1 kHz.

Above results suggest that Au/GO/PEDOT-PSS is a reliable, stable and sensitive electrode for capacitive biosensing applications. Incorporation of gold nanoparticles in GO/PEDOT-PSS had shown an increase in electron transfer and reactive species diffusion inside the porous polymer network. Moreover, the capacitive response changes almost instantly (< 1 min) upon antigen addition in the solution. This can be seen from the plot (Figure 2.11), where the change in capacitive trend has been appeared as vertically downward steps after addition of specific antigen. This resembles the fast response feature of the immunosensor. For Au/GO/PEDOT-PSS prototype capacitive sensor, the net change

in the capacitance value (ΔC_p) w.r.t. the concentration of antigen in the solution (after subsequent additions of antigen) is plotted in Figure 2.12 (a) and (b) for 77 Hz and 1 kHz, respectively. Here, the capacitive response increases rapidly in the concentration range of 10–38 ng/mL followed by a steady response beyond this concentration range and subsequent saturation. Figure 2.12 (b) shows the response of the sensor towards various concentrations of antigen at 1 kHz. Both the data points are fitted using the equation for adsorption isotherm, denoted as, $C_p = A\ (1 + B/[C])$; where, C_p is change in capacitive response, $[C]$ is change in antigen concentration. Here in the above equation, A is saturated capacitive response (C_{pm}) and B is the inverse of adsorption coefficient (k). The values of A and B are obtained from the fitted isotherm plot from Figure 2.12 (a) as 190.72 nF and 43.90 ng/mL respectively.

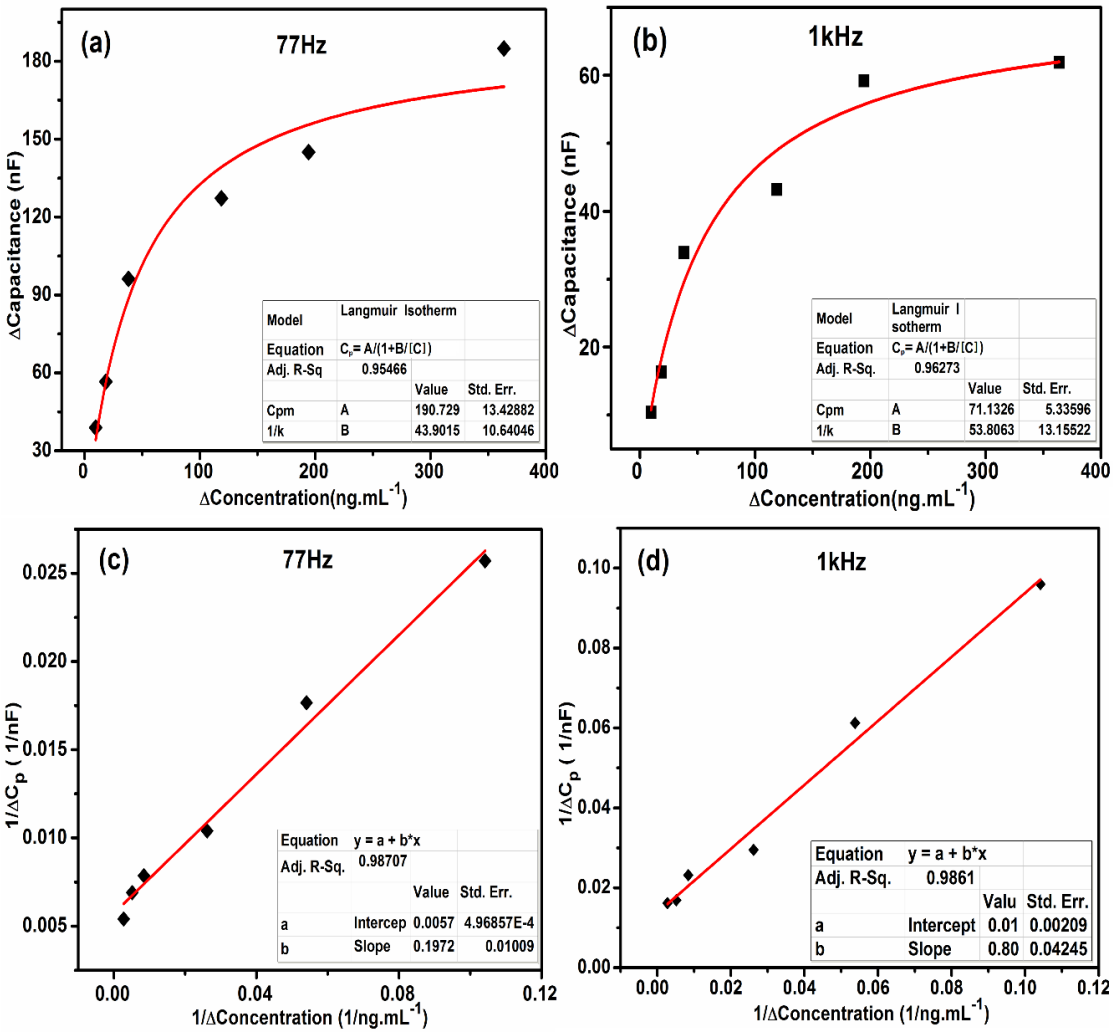

Figure 2.12: Change in capacitance vs. antigen concentration in AuNP/GO/ PEDOT-PSS sensor electrode at (a)77 Hz, and (b)1 kHz; (c) Linear regression fitting for 1/ (change in antigen concentration) vs. $1/\Delta C_p$ at 77 Hz, and (d) at 1 kHz.

From the fitted straight-line response of $1/(\Delta C_p)$ *vs.* $1/(\Delta[C])$ plots as given in Figure 2.12 (c) and (d), the limit of detection (*LOD*) was estimated as, 49 ng/mL and 47.4 ng/mL corresponding to the frequencies 77 Hz and 1 kHz, respectively. The calculation of *LOD* has been performed by using the formula, $LOD = \frac{3.3 \times \sigma_y}{m}$, [33] (see section 1.1.4) where; σ_y is the standard deviation of the *y*-intercept and *m* is the slope of the $1/(\Delta C_p)$ *vs.* $1/(\Delta[C])$ plot. We had also plotted transient conductance features of the Au/GO/PEDOTPSS sensor in Figure 2.13 (a) and (b) which also exhibits consistent electroactivity of the optimized electrode. However, the selectivity is poor in the absence of enzyme label as seen from the transient conductance change observed at both frequencies for addition of BSA. Therefore, we are highlighting the capacitance transient changes and selectivity to the specific antigen, especially in the case of label free capacitive sensors.

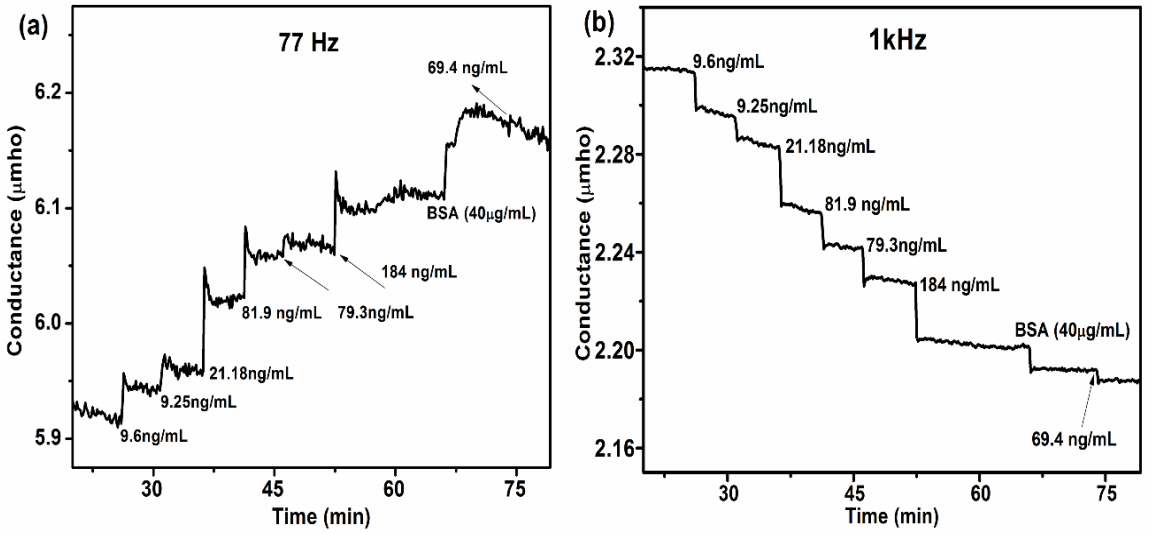

Figure 2.13: Conductance transient vs. time plot of Au/GO/PEDOT-PSS at (a) 77Hz, and (b) 1kHz

Another interesting observation from the electrochemical studies using the three types of electrodes for biosensing application was the better stability of the GO/Au incorporated PEDOT-PSS electrodes. We had physically observed that, part of the electrochemically polymerized PEDOT-PSS desorbs from the ITO surface mainly after antibody immobilization and subsequent washing step, as can be observed in Figure 2.14. It is known that the antibody molecules are high molecular weight (150 kD) protein molecules which may exert stress on the film surface.

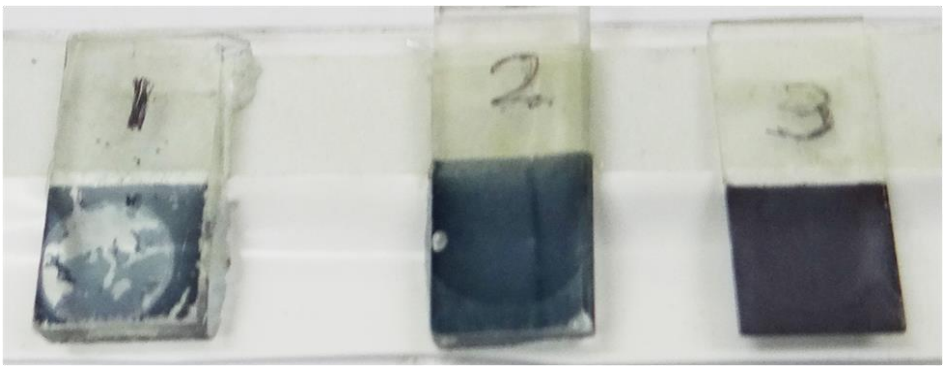

Figure 2.14: Photograph of the functionalized electrodes on ITO after sensing experiment (1) PEDOT-PSS, (2) GO/PEDOT-PSS, (3) Au/GO/ PEDOT-PSS

2.4 Conclusions

Composite thin film electrodes of GO/PEDOT-PSS and AuNP/GO/PEDOT-PSS have been prepared by user-friendly electrochemical methods and studied for label free, cost effective and selective biosensing applications. Detailed electrochemical studies of the composite electrodes suggested the change in charge transfer resistance and decrease in diffusion processes in the nanohybrid electrode after incorporation of GO and AuNPs in the polymer system. Afterwards, the electrodes were functionalized with glutaraldehyde to immobilize antibody at the electrode surface. Impedance studies of the hybrid electrodes after each process step of the immunosensor fabrication indicated qualitatively the electrochemical changes that could be occurring at the electrode/electrolyte interface. Direct measurements of antibody-antigen interaction using capacitance transient plot suggested that the immunosensor can exhibit a fast response towards the specific antigen (goat anti-mouse *IgG*) with a high sensitivity offering detection limits of 49 ng/mL for 77 Hz, and 47.4 ng/mL for 1 kHz signal frequency. The interesting feature of this work lies in its capacitive response based impedimetric detection technique that we have followed throughout sensing. Here, we proposed that the adsorption process taking place during the antibody antigen binding has followed the Langmuir adsorption isotherm. From there we have estimated the calibration curve for the immunosensor. The major limitation of this work is poor selectivity and moderate *LOD* of the sensor with low signal amplification. However, the complex analytical procedures that we have followed for estimating V_{fb} and choosing working frequency is challenging. These limitations demand further alteration in detection strategy along with consideration of technologically important materials.